10

Correlating structure with function in the viral capsid

MAVIS AGBANDJE-McKENNA AND MICHAEL S. CHAPMAN

THE MULTIFUNCTIONAL PARVOVIRUS COAT PROTEIN

The simple parvovirus capsid protein is capable of performing a wide variety of structural and biological functions during the viral life cycle. Sixty copies of a common sequence from this protein make up the capsid shell, with polypeptides VP1 to VP4 (depending on the virus) sharing identical C-terminal domains, but with decreasing overlapping regions. The entire sequence of VP4 (found only in members of the densovirus genus) is contained within VP3, that of VP3 is contained within VP2, and VP2 is contained within VP1, which in turn has a unique N-terminal extension. These viral coat proteins are translated from the same messenger RNA (mRNA) codons by the use of alternative splicing and non-consensus start codons. In the *Parvovirus* genus, for example, Kilman rat virus, canine parvovirus (CPV), feline panleukopenia virus (FPV), minute virus of mice (MVM) and porcine parvovirus (PPV), VP2 to VP3 cleavage is a capsid maturation step that occurs in full, but not in empty, particles following their release from the parental host cell (Tattersall *et al.*, 1977; Cotmore and Tattersall, 1987; Cotmore *et al.*, 1999; Maroto *et al.*, 2000). Following DNA packaging, 15–18 N-terminal residues are proteolytically cleaved from the N-termini of VP2 to generate VP3. This cleavage event is not observed in all parvovirus genera, for example, the *Amdovirus* genus, illustrated by Aleutian mink disease parvovirus (AMDV) or the *Erythrovirus* genus, illustrated by human parvovirus B19. These viruses contain only VP1 and VP2, translated from the same message using alternative start sites. For members of the *Dependovirus* and *Densovirus* genera, VP1, VP2, VP3, and VP4 are generated from overlapping RNA transcripts, and are not known to undergo a cleavage event. The VP1 capsid protein is always the minor component, while the smaller proteins, VP2, VP3, or VP4, depending on the virus, account for the highest percentage of the 60 copies of coat protein that make up the capsid.

The multitude of functional roles performed by the parvovirus capsid proteins includes host cell surface receptor recognition, pathogenicity determination, viral genomic encapsidation, self-assembly into capsids, maturation of virions to produce infectious virus progeny, nuclear import and export, escape from endosomes during infection, and host immune response detection and evasion. The relatively small parvoviral genome (~5000 ssDNA bases) has allowed the use of genetic manipulation to map functional domains of the viral proteins/capsid, which can be correlated to structural features of the particle.

Parvovirus capsids have been amenable to structural studies by X-ray crystallography and cryo-electron microscopy (cryo-EM). As detailed in the previous chapter (Chapter 9), high resolution 3D information is available for members of four main genera, namely *Parvovirus*, *Dependovirus*, *Erythrovirus*, and *Densovirus* (Tsao *et al.*, 1991; Agbandje *et al.*, 1993; Agbandje-McKenna *et al.*, 1998; Simpson *et al.*, 1998, 2000, 2002; Xie *et al.*, 2002; Govindasamy *et al.*, 2003; Kaufmann *et al.*, 2004). An 8 Å resolution structure is also

available for B19 determined by X-ray crystallography (Agbandje *et al.*, 1994). At lower resolution, the structure of *Junonia coenia* densovirus is available for the *Densovirus* genus (Bruemmer *et al.*, 2005); of empty capsids of adeno-associated virus (AAV) serotype 2 (Kronenberg *et al.*, 2001) and full capsids of AAV5 (Walters *et al.*, 2003) and AAV4 (Padron *et al.*, 2005) are available for the *Dependovirus* genus; of empty capsids of human parvovirus B19 (B19) made up of the major coat protein, VP2, and in complex with its infectious cellular receptor, globoside (Chipman *et al.*, 1996) are available for the *Erythrovirus* genus; of a CPV-Fab complex (Wikoff *et al.*, 1994) for the *Parvovirus* genus, and of VP2 capsids of AMDV (McKenna *et al.*, 1999) for the *Amdovirus* genus, determined using cryo-EM and image reconstruction.

The unique region of VP1, the minor parvovirus capsid protein, in addition to the VP2 N-termini, have proven refractory to structural elucidation possibly because of the symmetry constraints imposed during structural determinations, as described in Chapter 9. However, the amino acid sequences of these capsid protein regions play essential functional roles during the viral life cycle, and will be discussed briefly here. The unique region of VP1 displays a phospholipase A_2 (PLA_2) activity that is required for escape from late endosomes during viral trafficking to the nucleus after receptor mediated entry (Zádori *et al.*, 2001). In lieu of structural detail as part of the intact capsid, sequence analysis and model building exercises show that the PLA_2 domain within the VP1 N-terminus has a helical content consistent with known PLA_2 motifs (Zádori *et al.*, 2001). Despite low sequence homology to more conventional PLA_2 proteins, such as that in bee venom, the parvoviral PLA_2 sequences have the conserved catalytic and calcium binding sites required for this function (Zádori *et al.*, 2001). This unique VP1 region also contains basic amino acid clusters that function as nuclear localization signals (NLS), which direct nuclear import following entry and escape from the endosome (Vihinen-Ranta *et al.*, 2002). The PLA_2 and NLS functions are thought to be facilitated by the externalization of the VP1 unique peptide domains through pores at the icosahedral 5-fold axes (see Chapter 9) of the intact capsid. The exact mechanism of this externalization is still under intensive investigation but mutational studies of the MVM and AAV capsid proteins show that residues at the base and lining the 5-fold channel play essential roles in the PLA_2 function required for infectivity (Farr and Tattersall, 2004; Bleker *et al.*, 2005).

In parvoviruses that undergo VP2 to VP3 cleavage, the VP2 N-termini are also postulated to become externalized via the channels at the icosahedral 5-fold axes of their capsids (Tsao *et al.*, 1991; Xie and Chapman, 1996; Agbandje-McKenna *et al.*, 1998, Simpson *et al.*, 2002). Repulsion of phosphorylated VP2 N-terminal residues from the capsid interior following DNA packaging is thought to trigger this externalization, allowing their subsequent removal by cleavage of VP2 to VP3 (Maroto *et al.*, 2000). This process can be simulated in empty particles by heating to <70°C, while the capsids remain intact (Hernando *et al.*, 2000). The VP2 N-termini are also reported to facilitate nuclear export of newly-assembled parvovirus virions through interactions with the exportin molecule CRM1 (Maroto *et al.*, 2004).

The residues in the N-terminus of VP1, required for its PLA_2 function, and at the VP2 to VP3 cleavage site cannot be accommodated through the 5-fold channel without structural rearrangement of the surrounding β-ribbons, and immunological studies support the idea that this pore may 'breathe' (Cotmore *et al.*, 1999). However, once the VP1/2 N-termini have passed through the 5-fold channel, a glycine-rich sequence that is conserved in most parvoviruses can be accommodated within the channel (Xie and Chapman, 1996; Agbandje-McKenna *et al.*, 1998). Interestingly, while still able to accommodate a glycine-rich sequence, these channels are narrower in the B19 structure (Kaufmann *et al.*, 2004), consistent with the observation that B19 does not undergo VP2 to VP3 cleavage and that the VP1 unique region is always located on the capsid surface (Rosenfeld *et al.*, 1992).

The structure of the polypeptide sequence that is common to all the capsid proteins, which corresponds to VP2, VP3, or VP4 in viruses from different genera, is observed in a T = 1 icosahedral arrangement. The overall structural topology of this protein is the same for all parvoviruses (Figure 10.1A), even for pairs of viruses where amino acid sequence identity is only ~20 percent, as is observed, for example, between B19 and MVM (Chapman and Rossmann, 1993) and B19 and AAV2 (Kaufmann *et al.*, 2004; Padron *et al.*, 2005). The structural similarities between these viruses are ~70 percent, illustrating the greater conservation of tertiary structure compared with primary sequence. A CPV structure-based comparison of members of the *Parvoviridae* showed that the residues making up a core 8-stranded β-barrel motif (Figure 10.1A) and those lining the inner capsid surface are the most conserved. Surface loop residues inserted between the β-strands are the most varied (Chapman and Rossmann, 1993), and give rise to three types of surface topology (Figure 10.1B) (Xie *et al.*, 2002; Padron *et al.*, 2005). The most pronounced surface topology differences occur close to the icosahedral 2-fold axes and the protrusions surrounding the icosahedral 3-fold axes (Figure 10.1). Group 1 contains members of the *Parvovirus* genus, for example, CPV, FPV, MVM, and PPV, distinguished by a single pinwheel protrusion at the icosahedral 3-fold axes formed by loops contributed from three monomers, and a wider 2-fold depression. The *Densovirus* (DNV) capsid adopts a second topology, appearing relatively spherical with no large surface protrusions. The third group contains the AMDV, B19, AAV2, AAV4, and AAV5 capsids, which have three distinct mounds at a distance of ~20–26 Å from the icosahedral 3-fold axes, each mound resulting from the interaction of two 3-fold related monomers. The depression at their 2-fold axis also appears to be slightly deeper, particularly in B19 (Figure 10.1B).

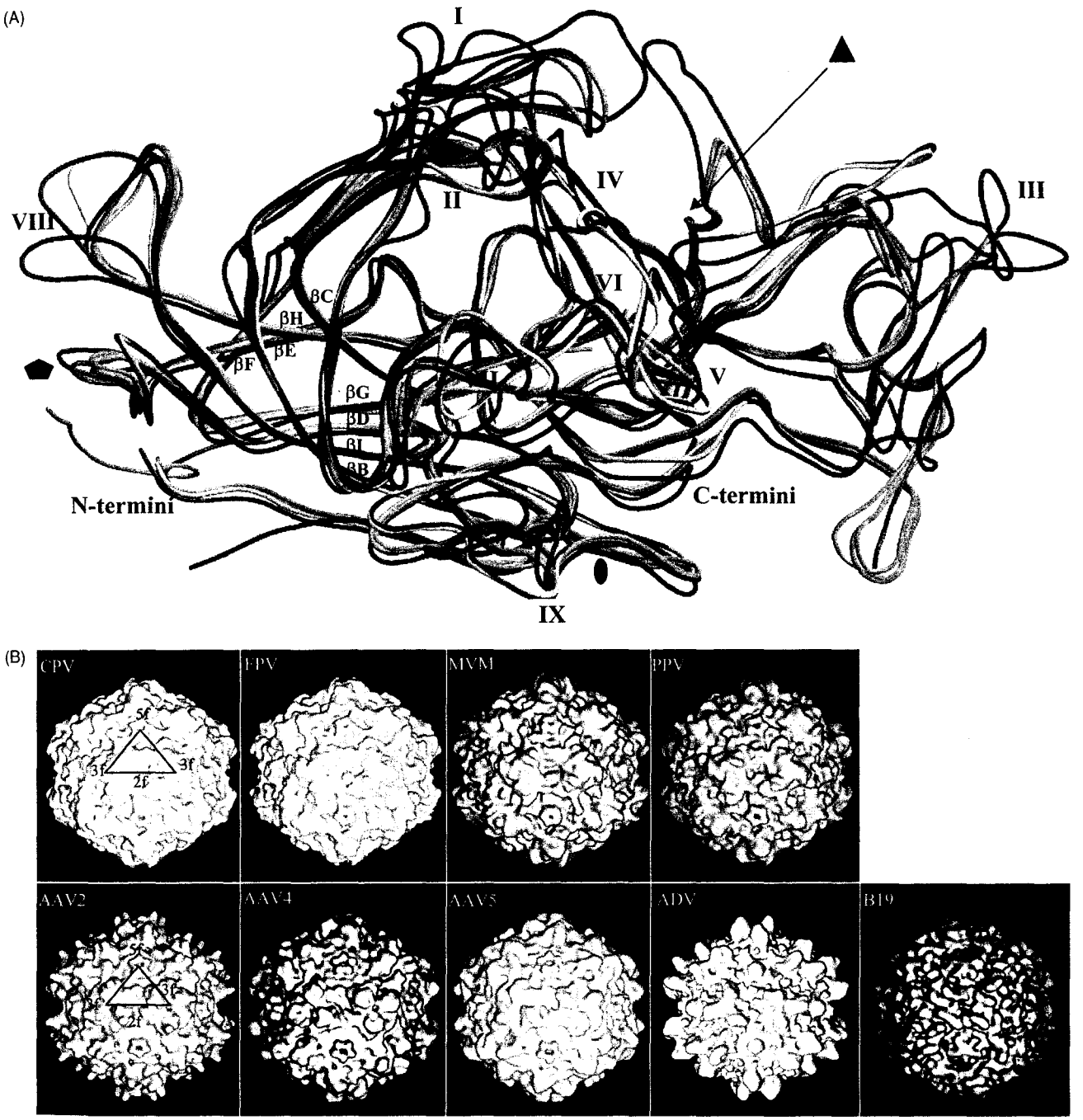

Figure 10.1 *Comparison of* parvovirus *structures. (A) Superimposition of coil representations of the VP2/VP3 monomers of AAV2 (brown), AAV4 (magenta), B19 (blue), CPV (orange), FPV (green), MVM (red), PPV (pink) (pdb accession Nos. 1LP3, AAV4 coordinates are yet to be deposited, 1S58, 2CAS, 1C8E, 1MVM, and IK3V), AAV5 (cyan) and ADV (grey) (pseudo-atomic model built into cryo-EM densities;* McKenna et al., *1999, Walters* et al., *2004). The most variable surface regions on the capsid are labeled (I–IX) as discussed by Padron* et al., *2005 and Govindasamy* et al., *2005. The eight-strands of the core β-barrel are labeled βB-βI. The approximate 2-fold (filled oval), 3-fold (filled triangle) and 5-fold (filled pentagon) axes are shown. This figure was generated using the program Bobscript (Esnouf, 1997). (B). Low resolution surface maps of AAV2, AAV4, AAV5, ADV, B19, CPV FPV, MVM, and PPV, at 13 Å resolution, colored as in (A). Viruses in the top panel and bottom panel form group I and group III, respectively in Padron* et al., *2005. The surface map images were generated as previously described (Belnap* et al., *1999) from atomic/pseudo-atomic coordinates as referenced in (A). The black triangles on the CPV and AAV2 capsid surfaces depict a viral asymmetric unit bound by a 2-fold (2f), two 3-folds (3f) and a 5-fold (5f) axis. See also Color Plate 10.1.*

The observed differences in the capsid surface features of the parvoviruses might be indicative of evolutionary changes that allow them to recognize and infect different hosts and host cells, and to evade host immune surveillance, while conservation of the β-barrel motif suggests a need to conserve core structural domains that may be required for assembly. However, there do not appear to be any unifying phenotypic similarities between parvoviruses with similar capsid surface topologies (Padron *et al.*, 2005). Viruses with similar surface topologies:

- do not necessarily recognize the same receptor molecules;
- do not necessarily have similar tissue tropisms and/or pathogenic phenotypes, and
- are not antigenically cross-reactive.

However, the *Amdovirus*, *Dependovirus* and *Parvovirus* capsids, regardless of local surface topology, utilize analogous capsid regions for these functions.

The structural information from the VP2/VP3/VP4 common region enables functional domains to be mapped onto the capsid. Slight structural variations in the capsid surface are known to modulate host cell tissue tropism, pathogenic disparities and antigenic differences between highly homologous strains (Parrish, 1991; Chang *et al.*, 1992; Agbandje *et al.*, 1993, 1995; Strassheim *et al.*, 1994; Wikoff *et al.*, 1994; Parker and Parrish 1997; Agbandje-McKenna *et al.*, 1998; Simpson *et al.*, 2000, 2002; Govindasamy *et al.*, 2003; Hueffer *et al.*, 2003a,b; Llamas-Saiz *et al.*, 1996; López-Bueno *et al.*, 2003; Palermo *et al.*, 2003). Surface regions also control variations in receptor attachment specificity between members of the same genus (Xie *et al.*, 2002; Govindasamy *et al.*, 2003; Hueffer *et al.*, 2003a,b; Kern *et al.*, 2003; Opie *et al.*, 2003). In addition, efforts to locate VP amino acids required for assembly have identified residues at the interface between icosahedral symmetry axes that suggest a role for both conserved and variable regions in the building of the parvovirus capsid (Carreira *et al.*, 2004; Reguera *et al.*, 2004; Bleker *et al.*, 2005). The capsid determinants of receptor attachment, tissue tropism and pathogenicity, and antigenicity will be discussed in the following sections.

RECEPTOR ATTACHMENT PHENOTYPES OF PARVOVIRUS CAPSIDS

Receptor-mediated attachment and entry are essential first steps in the parvoviral life cycle. Mutational and biochemical analysis, in combination with structural mapping, shows clearly that regardless of parvovirus genus or sequence homology, common regions of the capsid may be used to interact with carbohydrate moieties/receptor molecules during cell recognition and infection/transduction. However, these recognition sites are not restricted to a single feature or capsid region. The depression at the icosahedral 2-fold axis, the wall between the 2- and 5-fold depressions, the base of the 3-fold mound, and the icosahedral 3-fold axis have all been mapped as possible cell surface recognition sites. For most of these viruses, the recognition site is only configured on assembled capsids, and spatially distant sites on the capsid may be involved in the recognition of one receptor molecule, as reported for CPV (see below; Govindasamy *et al.*, 2003; Hueffer *et al.*, 2003a,b).

Cell transduction phenotypes for members of the *Dependovirus* genus appear to be due to the ability of different AAV capsids to use different cell surface carbohydrates for cell binding and entry. Heparin sulfate has been identified as the carbohydrate component important for AAV2 cell binding and transduction (Kern *et al.*, 2003; Opie *et al.*, 2003), with human fibroblast growth factor 1 (Qing *et al.*, 1999) or integrin $\alpha_v\beta_5$ acting as co-receptors (Summerford *et al.*, 1999). Amino acids R484, R487, K532, R585, and R588 are the basic residues in VP3 responsible for AAV2's interaction with heparin (Figure 10.2A). AAV1 does not contain critical residues R585 and R588 (Rabinowitz *et al.*, 2002), and does not bind heparin, although it is ~83 percent identical to AAV2. The carbohydrate moiety recognized by AAV1 for transduction is yet to be determined. AAV3 is ~87 percent identical to AAV2 and also lacks R585 and R588, but it binds heparin sulfate, albeit with lower affinity than AAV2 (Rabinowitz *et al.*, 2002). AAV4 and AAV5 are ~55 percent identical to AAV2 and to each other, and both use sialic acid rather than heparin sulfate for cellular transduction (Kaludov *et al.*, 2001). Platelet-derived growth factor receptor molecules, PDGFRa or PDGFRb, are also required as co-receptors to mediate AAV5 transduction (Di Pasquale *et al.*, 2003). The carbohydrate molecules mediating cell binding by other distinct AAV serotypes, such as AAV7–11 and avian adeno-associated virus (AAAV), are still under investigation.

Residues contributing to the heparin binding sites of AAV2 are clustered from 3-fold related VP3 molecules at the base of the mounds surrounding the icosahedral 3-fold axes (Xie *et al.*, 2002; Kern *et al.*, 2003; Opie *et al.*, 2003) (Figure 10.2A). Comparison of a cryo-EM reconstructed image of AAV4, at 13 Å resolution, with AAV2 at the same resolution, showed local surface structure variations proximal to this basic patch (Padron *et al.*, 2005). More recently, the crystal structure of AAV4 became available (Govindasamy *et al.*, 2005). Three of the five AAV2 residues that form the basic patch, including the critical R585 and R588, are different in AAV4, and the topology of loops forming this region of the 3-fold mounds are drastically different. In addition AAV4 has a deeper 2-fold depression because the loop containing K532, which lies on the wall of the 2-fold depression at the base of the 3-fold mound in AAV2, adopts a different conformation (Govindasamy *et al.*, 2005; Padron *et al.*, 2005). Comparisons of the AAV2 and AAV4 structures with a pseudo-atomic model of AAV5 built into its cryo-EM reconstructed density show that the major surface variations between all three viruses involve residues

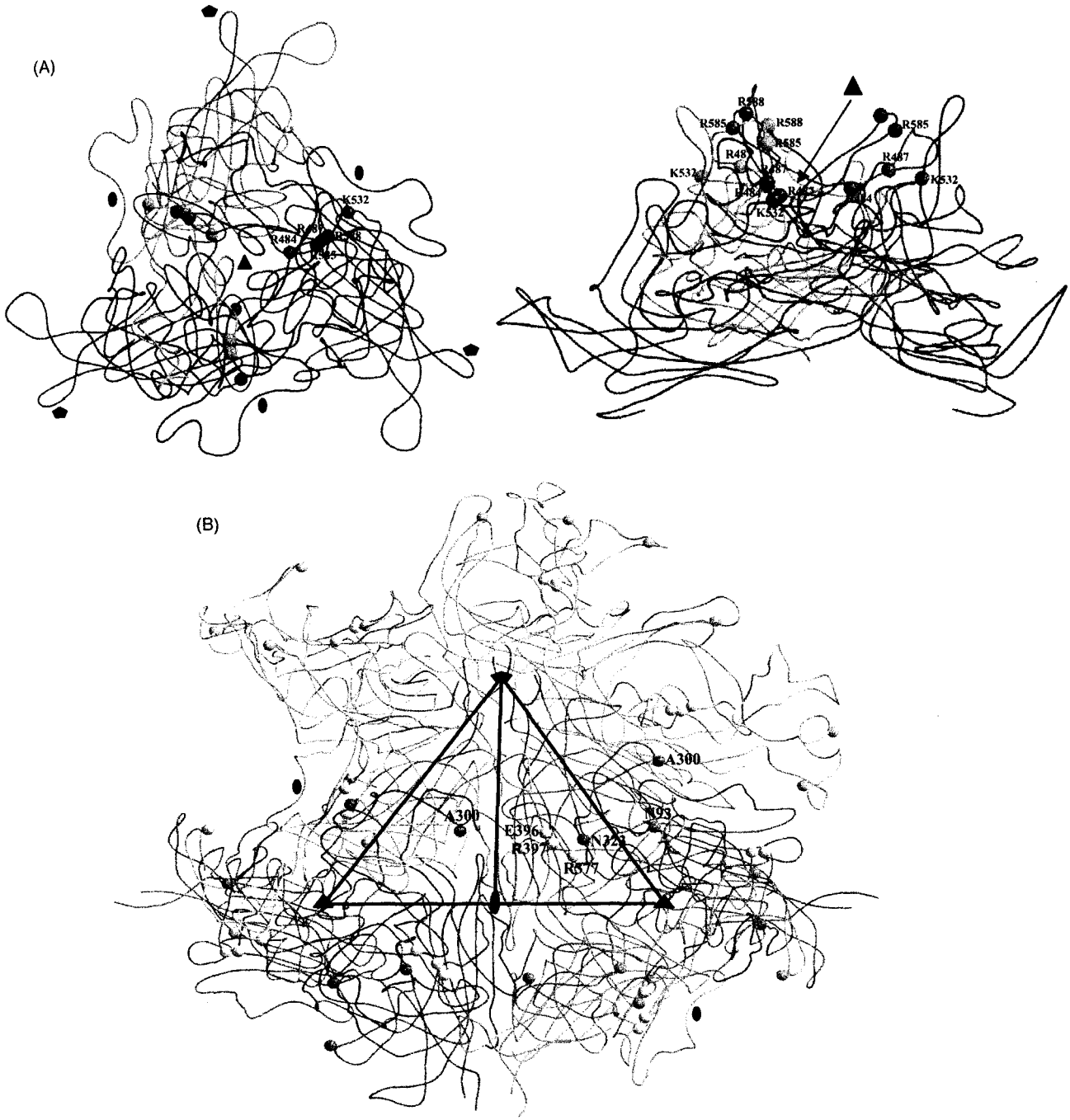

Figure 10.2 *Proposed receptor attachment sites on the AAV2 and CPV capsids. The coordinates were obtained as in Figure 10.1.* ***(A)*** *AAV2 VP3 trimer (monomers in brown, magenta and green) viewed down the icosahedral 3-fold axes (left-hand side) and rotated 90° (right-hand side). The Cα positions of residues R484, R487, K532, R585, and R588 (labeled and in the blue oval) that are clustered on the AAV2 capsid from 3-fold symmetry-related monomers to form a basic patch required for heparin sulfate binding are shown as balls colored according to their monomers. The approximate icosahedral 2-, 3-, and 5-fold axes are shown as the filled oval, triangle, and pentagons, respectively.* ***(B)*** *CPV VP2 reference (in orange) bounded by its icosahedral 2-fold (magenta), 3-fold (dark green and light green) and 5-fold (cyan) related monomers. The residues that control CPV sialic acid binding (R377, E396, and R397) on the wall of the 2-fold axes are shown in yellow balls in all monomers. The residues implicated in Tfr binding (93, 300, and 323) are shown in balls colored according to their contributing monomers. The approximate icosahedral 2- (filled oval), 3- (filled triangle), and 5-fold (filled pentagon) axes are shown. See also Color Plate 10.2.*

clustered at and around the 3-fold mounds, in the 2-fold depression, and on the floor of the depressions surrounding the icosahedral 5-fold axes. In addition, structural models generated for the other distinct AAV serotypes show a similar trend in surface variation (Padron *et al.*, 2005). There are no consensus sequences for sialic acid binding, but extrapolation from studies on CPV and MVM (see below) suggest that the icosahedral 2-fold axes may function as sialic acid binding regions. Thus the observed local surface loop variations between the AAV serotypes at the icosahedral 2- and 3-fold axes may control their abilities to recognize different carbohydrate components of cell surface receptors and play a role in their cellular transduction phenotypes.

B19, the best characterized member of the *Erythrovirus* genus, is known to have hemagglutinating activity (HA) that depends upon the non-sialated glycolpid globoside, which is its infectious cellular receptor (Brown *et al.*, 1993). Cryo-EM and image reconstruction showed this receptor binding in a depression at the viral icosahedral 3-fold axes (Chipman *et al.*, 1996). This 3-fold attachment site is proximal to the heparin-binding regions identified in AAV2 (Xie *et al.*, 2002; Kern *et al.*, 2003; Opie *et al.*, 2003). Despite the low sequence homology between B19 and the AAVs, their capsid topology is remarkably similar (Figure 10.1, p. 127) (Kaufmann *et al.*, 2004; Padron *et al.*, 2005). Whether or not this surface similarity results in the use of comparable capsid regions for receptor molecule(s) recognition remains to be determined by mutational analysis and structural studies of virus:receptor complexes.

The most extensively characterized members of the *Parvovirus* genus with respect to cell surface receptor attachment phenotype are CPV and FPV. Mutational and erythrocyte binding analysis of these viruses showed that they display a pH-dependent phenotype for binding (Chang *et al.*, 1992; Barbis *et al.*, 1992), and identified three amino acids residues, R377, R396, and E396, on the wall of the icosahedral 2-fold dimple-like depression (Figure 10.2B) that were required for HA (Tresnan *et al.*, 1995). These studies also identified sialic acid as the carbohydrate component of the receptor engaged in this interaction (Tresnan *et al.*, 1995). However, CPV and FPV do not replicate in erythrocytes, and thus the observed attachment most likely does not play a physiologically relevant role in the viral life cycle. In addition, a non-hemagglutinating mutant of CPV is able to productively infect susceptible host cells, indicating that sialic acid binding may not be a requirement or a component of the infectious receptor interaction (Tresnan *et al.*, 1995).

The infectious cell surface receptors for CPV and FPV have been identified as the canine and feline transferrin receptors (CTfR and TfR), respectively (Parker *et al.*, 2001, Palermo *et al.*, 2003). Further analysis clearly showed that the canine TfR controls CPV host range, facilitating the binding of CPV, but not FPV, capsids to canine cells (Hueffer *et al.*, 2003a,b). Mutational, binding and structural studies of CPV mutants identified three distinct regions of the capsid, involving residues 93, 300, and 323, as being responsible for CTfR binding (Govindasamy *et al.*, 2003; Hueffer *et al.*, 2003a,b). These loci, separated by up to 37 Å, are located on the capsid surface between the icosahedral 2-, 3- and 5-fold axes (Figure 10.2B) (Govindasamy *et al.*, 2003). Elucidating the nature of the contact(s) between these three capsid regions and the canine and feline TfR awaits the analysis of the structure of CPV and FPV with their respective receptor molecules.

The ability to bind cell surface sialic acid is a characteristic shared by several other parvoviruses, including bovine parvovirus (BPV), MVM, and PPV (Cotmore and Tattersall, 1987; Thacker and Johnson, 1998; López-Bueno *et al.*, 2005; Tijssen, personal communication). The BPV capsid is capable of binding to glycophorin A (Thacker and Johnson, 1998), a heavily sialylated protein found on erythrocyte membranes, although its infectious cell surface receptor is unkown. PPV's sialylated glycoprotein receptor is also yet to be identified. Similarly, the infectious receptor for MVM remains unknown but neuraminidase treatment of cells blocks attachment and inhibits infection (Cotmore and Tattersall, 1987; López-Bueno *et al.*, 2005), indicating that sialic acid is an essential carbohydrate component of its infectious cell surface receptor(s).

A crystallographic study of the prototype strain of MVM (MVMp) crystals soaked with sialic acid identified the icosahedral 2-fold as a possible carbohydrate binding site (López-Bueno *et al.*, 2005). This study represents the first visualization of a receptor component bound to a parvovirus capsid at high resolution. The binding site is proximal to the CPV residues 377, 396, and 397 (Figure 10.2B) that control its binding to sialic acid during erythrocyte hemagglutination (Tresnan *et al.*, 1995), as discussed above. The identification of this sialic acid binding site on MVMp and the mutations on CPV that inhibit sialic acid binding strongly point to the common use of the 2-fold depression as a binding site for this carbohydrate on the autonomous parvovirus capsid. The possible use of this binding site by members of the *Dependovirus* genus for sialic acid recognition remains to be assessed.

TISSUE TROPISM AND PATHOGENICITY DETERMINANTS

Members of the *Dependovirus* genus are non-pathogenic. The role of their major capsid protein, VP3, in tissue transduction is discussed above in relation to the types of carbohydrate moieties recognized as components of receptor molecules during infection. The role of the major *Densovirus* coat protein, VP4, in tissue tropism and pathogenicity is under investigation, and is not discussed in this chapter. For the *Erythrovirus* genus, comparisons of the available B19 capsid amino acid sequences have identified the VP1 unique region as the most variable locus, and thus the relationship of structure to tropism and pathogenicity differences remains to be determined.

For members of the *Parvovirus* and *Amdovirus* genera, pronounced *in vitro* tissue tropism and *in vivo* pathogenicity disparities between highly homologous strains are well documented (Hahn *et al.*, 1977; Engers *et al.*, 1981; Spalhotz and Tattersall, 1983; Tattersall and Bratton, 1983; Kimsey *et al.*, 1986; Alexandersen, 1990; Brownstein *et al.*, 1991, 1992; Segovia *et al.*, 1991, 1995, 1999; Chang *et al.*, 1992; Bloom *et al.*, 1993, 1998; Bergeron *et al.*, 1996; Maxwell *et al.*, 1995; Ramírez *et al.*, 1996). Host range and pathogenicity differences between highly homologous viruses might occur at various stages of the viral life cycle, including cell receptor attachment, viral entry, uncoating, DNA replication or transcription. For these viruses, particularly with AMDV, CPV/FPV, MVM, PPV as models, molecular analysis, *in vitro* and *in vivo*, shows that VP2/VP3, their major coat protein, plays a crucial role in tissue tropism and the onset of an *in vivo* pathogenic outcome following cell infection (Gardner and Tattersall, 1988a,b; Ball-Goodrich *et al.*, 1991; Ball-Goodrich and Tattersall, 1992; Brownstein *et al.*, 1992; Chang *et al.*, 1992; Bloom *et al.*, 1993, 1998; Parrish *et al.*, 1988; Parrish, 1991; Truyen *et al.*, 1994, 1996; Maxwell *et al.*, 1995; Fox *et al.*, 1999).

Two strains, AMDV-G and AMDV-Utah, which are approximately 97 percent identical in their VP2 sequence, have provided the viral models for probing host range and pathogenicity determinants in AMDV, a virus that can cause chronic and persistent diseases in mink (Bloom *et al.*, 1994). AMDV-G is a tissue culture-adapted strain that is non-pathogenic, while AMDV-Utah is highly pathogenic *in vivo* but does not grow in tissue culture. CPV and FPV cause an enteric disease in puppies and kittens, respectively, but are >99 percent identical at the DNA level and differ by only 9 or 10 out of 584 amino acids in their VP2 sequence (Parrish and Carmichael, 1986; Parrish *et al.*, 1988; Parrish, 1991). CPV and FPV can both replicate in cat cells *in vitro*, but only CPV can replicate in dogs and dog cells, although there are CPV variants, with capsid mutations, that can replicate *in vivo* in cats. FPV tropism in dog cells is restricted to selected tissues (Truyen *et al.*, 1994, 1996). The prototype and immunosuppressive strains of MVM, MVMp and MVMi respectively, also display disparate tropisms and pathogenic phenotypes despite the fact that their VP2 molecules are approximately 97 percent identical (Ball-Goodrich *et al.*, 1991). *In vitro*, MVMp replicates in mouse fibroblast cell lines, while MVMi replicates in mouse T lymphocytes and hematopoietic cell lineages. *In vivo*, MVMp infection of adult and newborn mice is asymptomatic, while MVMi causes a lethal infection (Kimsey *et al.*, 1986; Brownstein *et al.*, 1991, 1992; Segovia *et al.*, 1991, 1995, 1999; Ramírez *et al.*, 1996). PPV is a causative agent of reproductive failure in pigs (Dunne *et al.*, 1965; Mengeling and Cutlip, 1976). Several PPV strains can be distinguished by pronounced differences in their tissue tropism and *in vivo* pathology, although their VP2 proteins are approximately 99 percent identical (Molitor and Joo, 1990; Bergeron *et al.*, 1996). NADL-2 is the attenuated vaccine strain that is non-pathogenic, but can be lethal if injected *in utero*, while Kresse, IAF-A54, IAF-76 and NADL-8 are virulent forms (Cutlip and Mengeling, 1975; Mengeling and Cutlip, 1975; Kresse *et al.*, 1985; Choi *et al.*, 1987).

For AMDV, CPV, FPV, MVM, and PPV, changes at three or fewer amino acid positions, at any one time, appear to govern tropism and the pathogenic outcome of infection, as determined by site-directed mutagenesis, forward mutations, and chimeric viruses (Gardner and Tattersall 1988b; Parrish *et al.*, 1988, Ball-Goodrich *et al.*, 1991; Parrish, 1991; Ball-Goodrich and Tattersall, 1992; Chang *et al.*, 1992; Horiuchi *et al.*, 1994; Bergeron *et al.*, 1996; Parker and Parrish, 1997; Bloom *et al.*, 1998; Truyen *et al.*, 1994, 1996; Fox *et al.*, 1999; Hueffer *et al.*, 2003a,b). The VP2/VP3 residues that control host range and pathogenicity differences include the following: AMDV – 352, 395, 434, 534; CPV/FPV – 93, 323, 80, 564, 568; MVM – 317, 321, 399, 460, 553, 558, and PPV – 378, 383, 436. The available pseudo-atomic model of AMDV built into a cryo-EM reconstructed image and atomic structures of CPV, FPV, MVM, and PPV capsids enable these residues to be mapped onto the respective capsid (Figure 10.3) (Agbandje *et al.*, 1993; Llamas-Saiz *et al.*, 1996; Xie *et al.*, 1996; Agbandje-McKenna *et al.*, 1998; McKenna *et al.*, 1999; Simpson *et al.*, 2000, 2002; Govindasamy *et al.*, 2003). Despite local capsid surface differences, the majority of these tropism and pathogenicity determinants are similarly located on the capsids of AMDV, CPV/FPV, MVM, and PPV, on or close to the capsid surface, in the depression at the icosahedral 2-fold axes or the 'wall' that surrounds it (Figure 10.3B) and on the shoulders of the 3-fold protrusions (Figure 10.3C). PPV residue 436 is located on the top of the icosahedral 3-fold protrusion (Figure 10.2C); however, more recent data suggests that it plays a very minor role in determining PPV pathogenicity (Peter Tijssen, personal communication).

In all the viruses, the determinant residues are located throughout the primary amino acid sequence, but become clustered on the assembled 3D capsid (Figure 10.3). For example, FPV tropism and pathogenicity determinant residues 80, 564, and 568 are brought together on the shoulder of the 3-fold protrusions by a 5-fold symmetry operation (Truyen *et al.*, 1994, 1996; Govindasamy *et al.*, 2003). In MVM, forward mutation residues 399, 460, 553, and 558, that confer fibrotropism to MVMi are clustered in the 2-fold depression (Agbandje-McKenna *et al.*, 1998). A 3-fold symmetry operation locates the allotropic determinant residues 317 and 321 (Ball-Goodrich *et al.*, 1992) proximal to the 2-fold depression on the wall immediately above residues 399 and 460 in the depression (Figure 10.3C).

ROLE OF RECEPTOR RECOGNITION IN TISSUE TROPISM AND PATHOGENICITY

Cell binding and entry studies with CPV/FPV and MVM had shown that initial cell recognition/receptor attachment

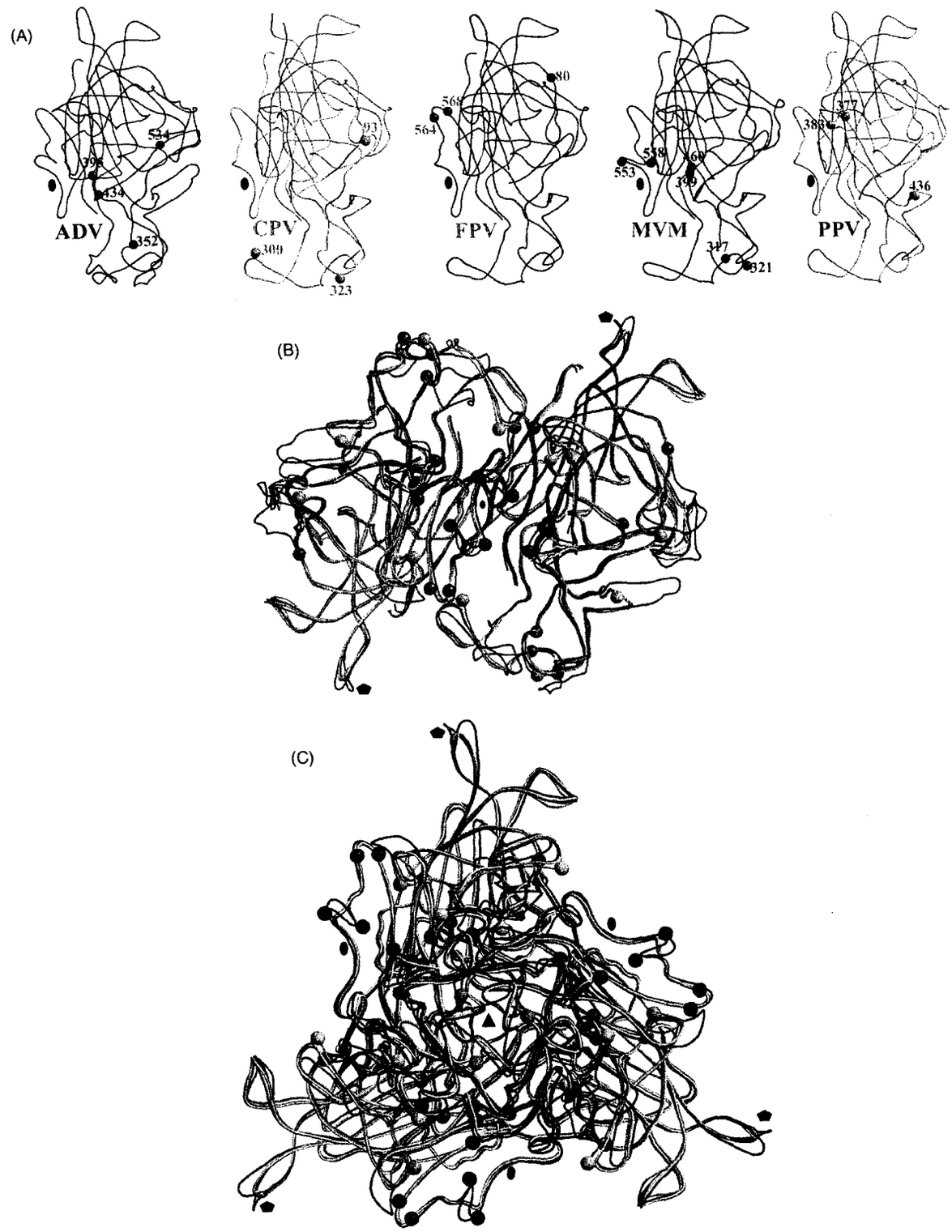

Figure 10.3 *Tissue tropism and pathogenicity determinants for members of the* Parvovirus *genus. (A) Coil representations of the VP2/VP3 monomers of ADV, CPV, FPV, MVM and PPV (generated from coordinates and colored as in figure 10.1A) viewed approximately down the icosahedral 2-fold axes. The Cα positions of residues implicated in tropism and pathogenicity determination are shown as balls and colored accordingly to the monomers. In MVM, forward mutations conferring fibrotropism to MVMi are in blue. (B) and (C) Superimposition of the monomers in (A) viewed down the icosahedral 2-fold and 3-fold axes, respectively. The tropism and pathogenicity/virulence determinants are colored as in (A) and clustered mainly in and around the depression at the icosahedral 2-fold axes. The approximate icosahedral 2- (filled oval), 3- (filled triangle), and 5-fold (filled pentagon) are shown. See also Color Plate 10.3.*

was not restricted in non-permissive cell lines and suggested that specific interactions with differentiation-dependent intracellular factor(s) in the permissive host cell, following initial entry, was required for replication to occur (Spalhotz and Tattersall, 1983; Gardner and Tattersall, 1988a). It was postulated that host range was controlled at this second interaction step (Spalhotz and Tattersall, 1983; Horiuchi *et al.*, 1992). Specifically, it was suggested that the block in restrictive cell lines occurred after entry and conversion of the genomic single-strand DNA to replicative form intermediates, but prior to viral genome transcription. However, structural co-localization of the critical *in vitro* tissue tropism and *in vivo* pathogenicity determinants with capsid surface residues that most likely control cell surface receptor recognition prompts re-evaluation of these earlier assumptions.

In the CPV/FPV system, residues 93 and 323 that are involved in differentiating the host range and *in vivo* pathogencity of CPV and FPV (Parrish *et al.* 1988; Parrish, 1991; Chang *et al.*, 1992) form part of the predicted TfR binding site. This site also involves residues in the 300 region that, in new strains of CPV, support mutations implicated in the host range control of CPV capsid binding by canine TfR (Parker and Parrish, 1997; Hueffer *et al.*, 2003a). The 300 region is also proximal to capsid residues 80, 564, and 568 that control FPV host range (Truyen *et al.*, 1994, 1996). In the MVMi/p system, residues 399, 460, 553, and 558, implicated in determining tissue tropism, are located in the vicinity of the sialic acid binding site recently identified in MVMp (López-Bueno *et al.*, 2005). Furthermore, an additional seven (of the 14) amino acids that vary between the VP2 sequence of MVMi and MVMp are clustered in this 2-fold region, with the allotropic determinants, 317 and 321, nearby on the shoulder of the protrusions at the icosahedral 3-fold axes that can also be considered as the wall of the 2-fold depression (Figure 10.3B and C) (Agbandje-McKenna *et al.*, 1998). For AMDV and PPV, tissue tropism and pathogenicity determinants are also located on or close to the capsid surface, in analogous regions to CPV/FPV and MVM. These observations point to a role for capsid surface interactions with primary cell surface receptor(s) in the differential tropism and pathogenicity of CPV and FPV, and of MVMi and MVMp, and such interactions may also modulate infection by AMDV and PPV strains (Agbandje-McKenna *et al.*, 1998; Simpson *et al.*, 2002; Govindasamy *et al.*, 2003; Hueffer *et al.*, 2003a,b; López-Bueno *et al.*, 2005).

ANTIGENIC PROPERTIES OF PARVOVIRUS CAPSIDS

Antibody binding can neutralize virus at various stages in the infectious process, including receptor attachment, trafficking and uncoating (Smith and Moser, 1997).The elaborate loop regions between the strands of the viral β-barrel, which make up the protrusions at or surrounding the icosahedral 3-fold axes, and form the walls between the depressions at the 2- and 5-fold axes, are the most immunogenic sites in the parvovirus capsid. For some members of the *Parvoviridae*, the available data suggest that neutralization can be mediated by more than one mechanism. Neutralizing epitopes have been mapped for members of the *Dependovirus*, *Erythrovirus* and *Parvovirus* genera, but not for the *Densovirus*. Many viruses, including members of the *Parvoviridae*, are known to sustain adaptive capsid mutations that enable them to escape antibody recognition and thus evade the immune response of their host. Members of the *Parvoviridae* for which escape mutants have been mapped include CPV and MVM. Significantly, the capsid surface structures of *Gm*DNV and JcDNV are not decorated with protrusions (Simpson *et al.*, 1998; Bruemmer *et al.*, 2005), possibly because these viruses are not exposed to a humoral immune response in their host. According to this scenerio, structural mutations and elaborations in the capsid surfaces that would allow them to evade an ongoing immune response have never been selected in the densoviruses, thus explaining their smoother architecture when compared with the vertebrate-infecting genera, which exhibit elaborate immunogenic loop decorations.

Antigenically, AAV2 is the best characterized member of the dependoviruses, since peptide mapping has been used to identify both linear and conformation-dependent epitopes on the capsid (Wistuba *et al.*, 1997; Wobus *et al.*, 2000). Three linear epitopes (A1, A69, and B1) and four conformational epitopes (A20, C24-B, C37-B, and D3) have been reported, although the residues for the C24-B site have not been mapped. For the linear epitopes, A1 recognizes VP1 only, while A69 recognizes a peptide in the VP1/VP2 common region, and B1 recognizes all three capsid proteins via an epitope at their C-termini (Wobus *et al.*, 2000). Antibodies to the conformation-dependent epitopes provide clear evidence that there are multiple mechanisms for parvoviral capsid neutralization. Thus, the C24-B and C37-B epitopes elicit antibodies that neutralize by inhibiting receptor attachment, while antibodies to the A20 site neutralize at a postattachment step, and D3 antibodies are non-neutralizing. Localization of the C37-B epitope (Figure 10.4A, residues 493–502, 601–610, VP1 numbering) close to the heparin binding site on the capsid is consistent with its function. Antibodies to the C37-B epitope specifically recognize AAV2, and not AAV1, 3, 4, or 5, in keeping with the observation that surface loops close to the heparin binding region are the most variable when the capsid structures of AAV2, AAV4, and AAV5 are compared (Govindasmy *et al.*, 2005; Padron *et al.*, 2005). The D3 epitope (Figure 10.4A, residues 474–483) is fairly conserved in the sequences of most AAV serotypes (Padron *et al.*, 2005), but D3 antibodies recognize serotypes AAV1, 3 and 5, not 4. This observation is consistent with these residues being close to structural differences between AAV2 and AAV4 at the mounds surrounding the icosahedral 3-fold axes (Govindasamy *et al.*, 2005; Padron *et al.*, 2005). AAV serotype reactivity to the A20 antibody

is limited to AAV2 and AAV3. This epitope (Figure 10.4A, residues 272–281, 369–378 and 566–575) maps to three different regions in the primary sequence (Wobust *et al.*, 2000) that come together in the wall between the 2-, 3-, and 5-fold axes in the AAV2 capsid structure (Xie *et al.*, 2002). Superimposition of the AAV4 and AAV5 VP3 coat protein structures, obtained by X-ray crystallography and cryo-EM and image reconstruction (Govindasamy *et al.*, 2005; Walters *et al.*, 2004; Padron *et al.*, 2005), onto the X-ray structure of AAV2 VP3, identified these regions as some of the most variable between the three viruses. The AAV4 capsid also has the unique phenotype of not being recognized by the B1 antibody, which is directed to a linear epitope (residues 726–733) at the extreme C-terminal end of the AAV VP3 protein (Wobus *et al.*, 2000). Comparison of the AAV2 and AAV4 VP3 crystal structures at the B1 epitope amino acids showed no major conformation differences, with the Cα atoms being superimposable, suggesting that the histidine residue in AAV4, where all other AAVs so far identified have an arginine or lysine, is involved in the capsid antibody interaction (Govindasamy *et al.*, 2005). However, considering that a single amino acid change on a viral surface is able to ablate antibody recognition (Llamas-Saiz *et al.*, 1996), it is perhaps not surprising that AAV4 and AAV5 are not recognized by A20 and that AAV4 is not recognized by B1.

Antigenic epitopes on the highly immunogenic AMDV capsid have been mapped with peptides (Bloom *et al.*, 1997, 2001; McKenna *et al.*, 1999) to capsid regions similar to those described for AAV and CPV/FPV (see below), located on the wall between the 2-, 3-, and 5-fold axes, and on the inner wall of its 3-fold mounds. Interestingly, binding of antibodies to the AMDV capsid tends to result in immune enhancement of infection (ADE), rather than neutralization, a phenomenon that is unique to AMDV in the *Parvoviridae* family and is an important component of its disease mechanism. However, *in vitro*, an antibody directed against VP2 residues 428–446 (Figure 10.4B, in the wall of the 2-fold depression), which is capable of eliciting antibody-dependent enhancement, antibody-dependent enhancement (ADE), is able to neutralize infectivity in CrFK cells. This capsid region includes residue 434 (Figure 10.3) that is implicated in AMDV host range and pathogenicity, as discussed above. Another well characterized AMDV antigenic epitope, residues 487–501 (Figure 10.4B), is capable of inducing ADE, but is not neutralizing. This epitope is located on the inner wall of the mounds at the icosahedral 3-fold axes. Thus if interactions between the capsid and its receptor molecule define the tissue tropism and pathogenicity of highly homologous strains, as suggested above, the neutralization of AMDV by an antibody to the 428–446 epitope could be due to steric hindrance of receptor attachment.

Neutralizing epitopes on the erythrovirus B19 capsid have been mapped to the VP1 unique region and to the VP1/VP2 overlapping sequence (Sato *et al.*, 1991a,b; Yoshimoto *et al.*, 1991; Brown *et al.*, 1992; Rosenfeld *et al.*, 1992; Saikawa *et al.*, 1993). Most of the VP1/VP2 neutralizing epitopes are located on the loops that make up the protrusions on the B19 capsid surface (Figure 10.4C) (Sato *et al.*, 1991a,b; Yoshimoto *et al.*, 1991; Brown *et al.*, 1992; Kaufmann *et al.*, 2004). Antibodies that recognize VP2 residues 57–77, 345–365, and 446–466 are reported to inhibit HA by B19 (Brown *et al.*, 1993), while those generated for peptides from residues 253–515 (Figure 10.4C, epitope residues 253–272, 309–330, 325–346, 359–382, 449–468, and 491–515) are neutralizing. Mapping these residues onto the crystal structure of B19 (Kaufmann *et al.*, 2004) identifies residues 57–77, 253–272, 314–330, 325–346, and 359–382 on the wall between the 2- and 5-fold depressions and at the base of the 3-fold protrusions. The loop containing residues 309–313 is disordered in the B19 structure (Kaufmann *et al.*, 2004) but residues 314–330 structurally superimpose onto a portion of the AAV2 C37-B epitope (Figure 10.4C). Thus if the infectious receptor attachment site in B19 does co-localize with the heparin sulfate binding site of AAV2, as suggested (Kaufmann *et al.*, 2004), inhibition of receptor attachment would be a possible mechanism for neutralization by the antibody to this peptide. Residues 449–468 and 491–515 are located inside the assembled capsid, so neutralization by antibodies directed against these sites would have to occur after host cell entry or prior to capsid assembly.

Antigenic regions of the CPV and FPV capsids, mapped using peptide mapping and natural escape mutant analysis, also encompass the capsid surface ridges between the 2-fold and 5-fold depressions, the 'shoulder' of the 3-fold protrusions, regions close to the top of the 3-fold protrusions, residues that form the β-ribbons at the 5-fold axes and the VP1 unique region (Rimmelzwaan *et al.*, 1990; Lopez de Turiso *et al.*, 1991; Chang *et al.*, 1992; Cortés *et al.*, 1993; Langeveld *et al.*, 1993, 1994; Strassheim *et al.*, 1994). Two dominant immunogenic regions of the CPV/FPV capsid, referred to as epitope A and B (Figure 10.4D) and associated, in selected escape mutants, with mutations in VP2 residues 93, 222, 224, and 426, and 299, 300, 302, and 305, respectively, are located on the shoulder of the 3-fold protrusions and on the wall between the icosahedral 2- and 5-fold axes, respectively (Strassheim *et al.*, 1994; Agbandje *et al.*, 1995). Natural variants of CPV exist that are also resistant to monoclonal antibodies directed against epitope B. Cryo-EM and image reconstruction of CPV complexed with Fab fragments from a monoclonal antibody to epitope B identified an antibody footprint as previously mapped by sequence analysis of capsid neutralization escape mutations (Wikoff *et al.*, 1994). The capsid region surrounding and including epitopes A and B, show the greatest structural variation between CPV and FPV, and their host range and antigenic mutants (Agbandje *et al.*, 1993; Llamas-Saiz *et al.*, 1996; Simpson *et al.*, 2000; Govindasamy *et al.*, 2003). Residue 93 in epitope A and 299 and 300 in epitope B, plus a third capsid region containing residue 323 that is also immunogenic, are involved in host range determination for CPV and FPV and form the large footprint proposed as the TfR recognition site (Govindasamy *et al.*, 2003). Thus the mechanism

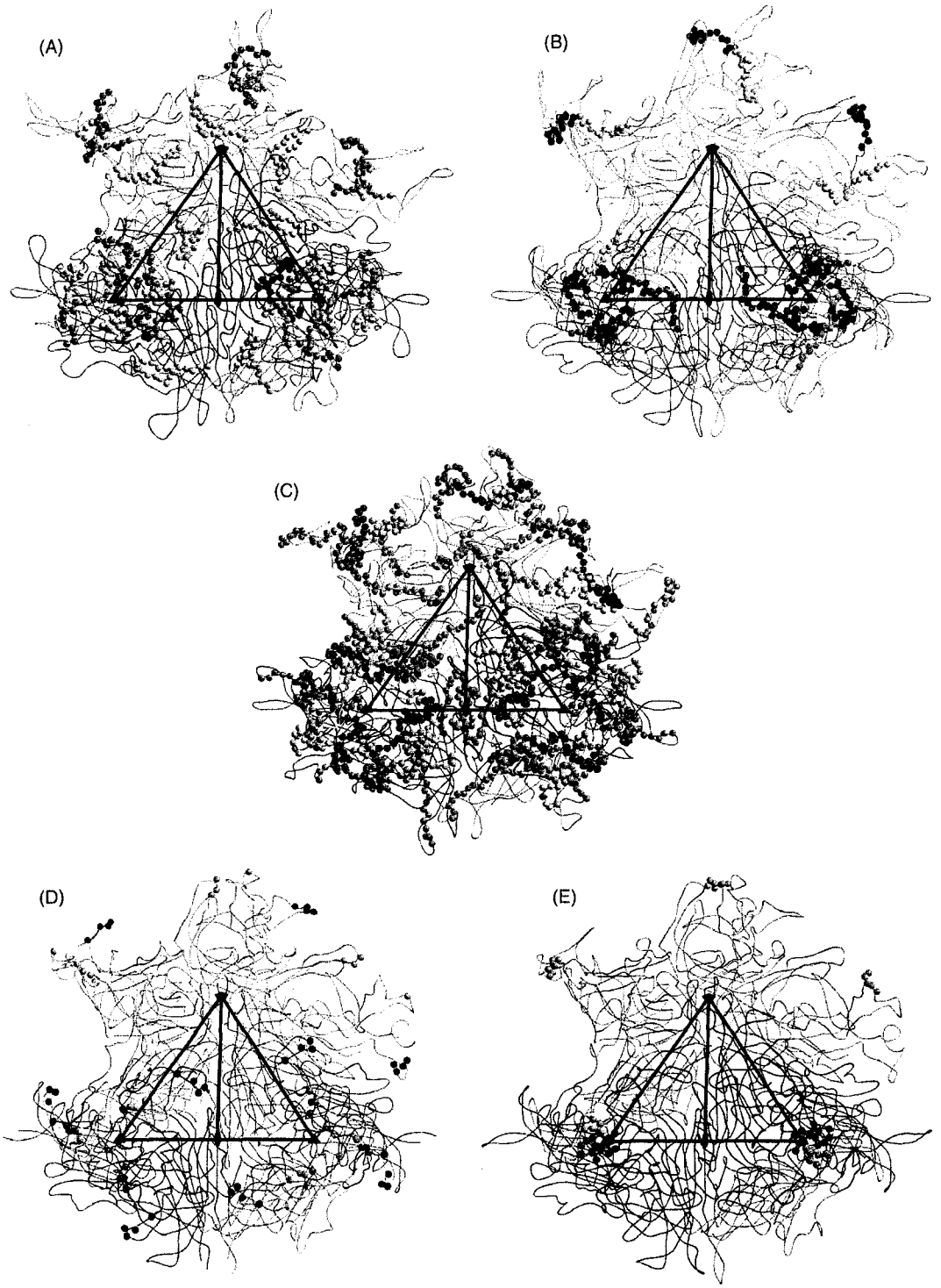

Figure 10.4 *Antigenic regions on parvovirus capsids. Antigenic regions on the AAV2 (**A**), ADV (**B**), B19 (**C**), CPV (**D**), and MVM (**E**) capsids are shown for the reference monomers (colored as in Figure 10.1) bounded by their icosahedral 2-fold (magenta), 3-fold (dark green and light green) and 5-fold (cyan) related monomers. For AAV2 (**A**), the Cα positions for the A20 epitope (VP1 numbering residues 272–281, 369–378, and 566–575) is shown in greenish yellow, the C37-B (residues 493–502 and 601–610) in pink and D3 (residues 474–483) in orange. The ADV (**B**) epitope at VP2 residues 428–446 is shown colored according to the monomers and the 487–501 epitope is colored in purple. The B19 (**C**) VP2 epitopes are colored as follows: 57–77 (pink); 253–272 (orange); 314–330 (part of 309–330) (red); 359–382 (yellowish green); 449–468 and 491–515 (grey). In CPV (**D**) antigenic epitope A (residues 93, 222, 224, and 426) is colored according to the monomers and epitope B (residues 299, 300, 302, and 305) is in grey. In MVM (**E**) escape mutant residues are shown in balls colored according to the monomers. The approximate icosahedral 2- (filled oval), 3- (filled triangle), and 5-fold (filled pentagon) axes are shown in A-E for a viral asymmetric unit. See Color Plate 10.4.*

for neutralization of viral infection by antibodies to these regions is likely the steric hindrance of receptor attachment, mediated by blocking essential residues that are required for specific interactions.

Escape mutants have also been reported for MVM, arising during long-term, passive, monoclonal antibody therapy in mice with severe immunodeficiency (SCID) (López-Bueno *et al.*, 2003). The mutant viruses that were able to escape neutralization, and which gave disease symptoms similar to the wild-type virus infection, contained single amino acid changes at VP2 amino acid positions 433–439, located in a surface loop at the very center of the protrusions at the icosahedral 3-fold axes (Figure 10.4E). Three such loops are located at the top of the 3-fold protrusions on the MVM capsid. The mechanism of neutralization by the antibodies to this epitope at the icosahedral 3-fold axes of MVM is unknown.

SUMMARY

Despite the apparent simplicity of the T = 1 parvovirus capsid, the proteins forming the protective coat around the parvovirus genome are capable of performing, or engaging the partners necessary for performing, the numerous interactions required for the propagation of progeny. While local capsid surface differences have produced three general parvovirus capsid topology groups, the functional regions co-localize to similar surface regions. The available 3D information for members of four main parvovirus genera, combined with the amenability of the parvoviral ssDNA genome to mutational analysis, has enabled the annotation and visualization of functional domains that play essential roles in the viral life cycle, particularly receptor attachment, *in vitro* tropism and *in vivo* pathogenicity, and antigenicity. A basic understanding of these phenotypes and the mapping of essential capsid sequences onto the capsid structure is a necessary step for infection and disease control, and will allow the genetic manipulation of parvovirus capsids for applications directed at developing foreign antigen and gene delivery systems.

REFERENCES

Agbandje, M., McKenna, R., Rossmann, M. G., Strassheim, M. L. and Parrish, P. R. 1993. Structure determination of feline panleukopenia virus empty particles. *Proteins* **16**: 155–71.

Agbandje, M., Kajigaya, S., McKenna, R., Young, N. S. and Rossmann, M. G. 1994. The structure of human parvovirus B19 at 8 Å resolution. *Virology* **203**: 106–15.

Agbandje-McKenna, M., Parrish, C. R. and Rossmann, M. G. 1995. The structure of parvoviruses. *Seminars in Virology* **6**: 299–309.

Agbandje-McKenna, M., Llamas-Saiz, A. L., Wang, F., Tattersall, P. and Rossmann, M. G. 1998. Functional implications of the structure of the murine parvovirus, minute virus of mice. *Structure* **6**: 1369–81.

Alexandersen, S. 1990. Pathogenesis of disease caused by Aleutian mink disease parvovirus. *Acta Pathologica, Microbiologica et Immunologica Scandinavica.* **98**: 1–32.

Ball-Goodrich, L. J., Moir, R. D. and Tattersall P.1991. Parvoviral target cell specificity: acquisition of fibrotropism by a mutant of the lymphotropic strain of minute virus of mice involves multiple amino acid substitutions within the capsid. *Virology* **184**: 175–86.

Ball-Goodrich, L. J. and Tattersall, P. 1992. Two amino acid substitutions within the capsid are coordinately required for acquisition of fibrotropism by the lymphotropic strain of minute virus of mice. *Journal of Virology* **66**: 3415–23.

Barbis, D. P., Chang, S.-F. and Parrish, C. R. 1992. Mutations adjacent to the dimple of the canine parvovirus capsid structure affect sialic acid binding. *Virology* **191**: 301–8.

Bergeron, J., Hébert, B. and Tijssen, P. 1996. Genome organization of the Kresse strain of porcine parvovirus, identification of allotropic determinant and comparison with those of NADL2 and field isolates. *Journal of Virology* **70**: 2508–15.

Belnap, D. M., Kumar, A., Folk, J. T., Smith, T. J. and Baker, T. S. 1999. Low-resolution density maps from atomic models: How stepping 'Back' can be a step 'Forward'. *Journal of Structural Biology* **125**: 166–75.

Bleker, S., Sonntag, F. and Kleinschmidt. 2005. Mutational analysis of narrow pores at the fivefold symmetry axes of adeno-associated virus type 2 capsids reveals a dual role in genome packaging and activation of phopholipase A2 activity. *Journal of Virology* **79**: 2528-2540.

Bloom, M. E., Berry, B. D., Wei, W., Perryman, S. and Wofinbarger, J. B. 1993. Characterization of chimeric full-length molecular clones of Aleutian mink disease parvovirus (ADV): identification of a determinant governing replication of ADV in cell culture. *Journal of Virology* **67**: 5976–88.

Bloom, M. E., Kanno, H., Mori, S. and Wolfinbarger, J. B. 1994. Aleutian mink disease parvovirus: puzzles and paradigms. *Infectious Agents and Diseases* **3**: 279–301.

Bloom, M. E., Martin, D. A., Oie, K. L. *et al.* 1997. Expression of Aleutian mink disease parvovirus capsid proteins in defined segments: localization of immunoreactive sites and neutralizing epitopes to specific regions. *Journal of Virology* **71**: 705–14.

Bloom, M. E., Fox, J. M., Berry, B. D., Oie, K. L. and Wolfinbarger, J. B. 1998. Construction of pathogenic molecular clones of Aleutian mink disease parvovirus that replicate both *in vivo* and *in vitro*. *Virology* **251**: 288–96.

Bloom, M. E., Best, S. M., Hayes, S. F. *et al.* 2001. Identification of aleutian mink disease parvovirus capsid sequences mediating antibody-dependent enhancement of infection, virus neutralization and immune complex formation. *Journal of Virology* **75**: 11116–27.

Brown, C. S., Jensn, T., Meloen, R. H. *et al.* 1992. Localization of an immunodominant domain on baculovirus-produced parvovirus B19 capsids: correlation to a major surface region on the native virus particle. *Journal of Virology* **66**: 6989–96.

Brown, K. E., Anderson, S. M. and Young, N. S. 1993. Erythrocyte P antigen: cellular receptor for B19 parvovirus. *Science* **262**: 114–17.

Brownstein, D. G., Smith, A. L., Jacoby, R. O., Johnson, E. A., Hansen, G. and Tattersall, P. 1991. Pathogenesis of infection with a virulent

allotropic variant of minute virus of mice and regulation by host genotype. *Laboratory Investigations* **65**: 357–63.

Brownstein, D. G., Smith, A. L., Johnson, E. A., Pintel, D. J., Naeger, L. K. and Tattersall, P. 1992. The pathogenesis of infection with minute virus of mice depends on expression of the small nonstructural protein NS2 and on the genotype of the allotropic determinants VP1 and VP2. *Journal of Virology* **66**: 3118–24.

Bruemmer, A., Scholari, F., Lopez-Ferber, M., Conway, T. F. and Hewat, E. A. 2005. Structure of an insect parvovirus (*Junonia coenia* dependovirus) determined by cryo-electron microscopy. *Journal of Molecular Biology* **347**: 791–801.

Carreira, A., Menéndez, M., Reguera, J., Almendral, J. M. and Mateu, M. G. 2004. *In vitro* disassembly of a parvovirus capsid and effect on capsid stability of heterologous peptide insertions in surface loops. *Journal of Biological Chemistry* **279**: 6517–25.

Chang, S.-F., Sgro, J. Y. and Parrish, C. R. 1992. Multiple amino acids in the capsid structure of canine parvovirus coordinately determine the canine host range and specific antigenic and hemagglutination properties. *Journal of Virology* **66**: 6858–67.

Chapman M. and Rossmann M. G. 1993. Structure, sequence and function correlations among parvoviruses. *Virology* **194**: 491–508.

Chipman, P. R., Agbandje-McKenna, M., Kajigaya, S. *et al.* 1996. Cryo-electron microscopy studies of empty capsids of human parvovirus B19 complexed with its cellular receptor. *American Journal of Veterinary Research* **93**: 7502–6.

Choi, C. S., Molitor, T. W., Joo, H. S. and Gunther, R. 1987. Pathogenicity of a skin isolate of porcine parvovirus in swine fetuses. *Veterinary Microbiology* **15**: 19–29.

Cortes, E., San Martin, C., Langeveld, J. *et al.* 1993. Topographical analysis of canine parvovirus virions and recombinant VP2 capsids. *Journal of General Virology* **74**: 2005–10.

Cotmore, S. and Tattersall, P. 1987. The autonomously replicating parvoviruses of vertebrates. *Advances in Virus Research* **33**: 91–174.

Cotmore, S. F., D-Abramo, A. M., Jr., Ticknor, C. M. and Tattersall, P. 1999. Controlled conformational transitions in the MVM virion expose the VP1 N-terminus and viral genome without particle disassembly. *Virology* **254**: 169–81.

Cutlip, R. C. and Mengeling, W. L. 1975. Pathogenesis of *in utero* infection: experimental infection of 8- and 10-week-old porcine fetuses with porcine parvovirus. *American Journal Veterinary Research* **36**: 1751–4.

Di Pasquale G., Davidson, B. L., Stein, C. S. *et al.* A. 2003. Identification of PDGFR as a receptor for AAV-5 transduction. *Nature Medicine* **9**: 1306–12.

Dunne, H. W., Gobble, J. C., Hokanson, J. R., Kradel, D. C. and Bubash, G. R. 1965. Porcine reproductive failure associated with a newly defined 'SMEDI' group of picornaviruses. *American Journal Veterinary Research* **26**: 1284–90.

Engers, H. D., Louis, J. A., Zubber, R. H. and Hirt, B. 1981. Inhibition of T cell-mediated functions by MVM(i), a parvovirus closely related to minute virus of mice. *Journal of Immunology* **127**: 2280–5.

Esnouf, R. 1999. BOBSCRIPT. Further additions to MOLSCRIPT version 1.4, including reading and contouring of electron-density maps. *Acta Crystallographica* **D55**: 938–40.

Farr, G. A. and Tattersall, P. 2004. A conserved leucine that constricts the pore through the capsid fivefold cylinder plays a central role in parvoviral infection. *Virology* **323**: 243–56.

Fox, J. M., McCrackin Stevenson, M. A. and Bloom, M. E. 1999. Replication of Aleutian mink disease parvovirus *in vivo* is influenced by residues in the VP2 protein. *Journal of Virology* **73**: 8713–19.

Gardner, E. M. and Tattersall, P. 1988a. Evidence that developmentally regulated control of gene expression by a parvoviral allotropic determinant is particle mediated. *Journal of Virology* **62**: 1713–22.

Gardner, E. M. and Tattersall, P. 1988b. Mapping of the fibrotropic and lymphotropic host range determinants of the parvovirus minute virus of mice. *Journal of Virology* **62**: 2605–13.

Govindasamy, L., Hueffer, K., Parrish, C. R. and Agbandje-McKenna, M. 2003. Structures of host range-controlling regions of the capsids of canine and feline parvoviruses and mutants. *Journal of Virology* **77**: 12211–21.

Govindasamy, L., Padron, L., McKenna, R., Kaludov, N., Muzyczka, N. Chiorini, J. A. and Agbandje-McKenna, M. 2005. Functional implications of the high resolution structure of adeno-associated virus serotype 4. *Proceedings of the National Academy of Sciences USA* (in preparation).

Hahn, E., Ramos, C. L. and Kenyon, A. J. 1977. Expression of Aleutian mink disease antigen in cell culture. *Infection and Immunity* **15**: 204–11.

Hernando, E., Llamas-Saiz, A. L., Foces-Foces, C. *et al.* 2000. Biochemical and physical characterization of parvovirus minute virus of mice virus-like particles. *Virology* **267**: 299–309.

Horiuchi, M., Ishiguro, N., Goto, H. and Shinagawa, M. 1992. Characterization of the stage(s) in the virus replication cycle at which the host-cell specificity of the feline parvovirus subgroup is regulated in canine cells. *Virology* **189**: 600–8.

Horiuchi, M., Goto, H., Ishiguro, N. and Shinagawa, M. 1994. Mapping of determinants of the host range for canine cells in the genome of canine parvovirus using canine parvovirus/mink enteritis virus chimeric viruses. *Journal of General Virology* **75**: 1319–28.

Hueffer, K., Govindasamy, L., Agbandje-McKenna, M. and Parrish, C. 2003a. Combinations of two capsid regions control host range and specific transferrin receptor binding by canine parvovirus. *Journal of Virology* **77**: 10099–105.

Hueffer, K., Parker, J. S., Weichert, W. S., Geisel, R. E., Sgro, J. Y. and Parrish, C. R. 2003b. The natural host range shift and subsequent evolution of canine parvovirus resulted from virus-specific binding to the canine transferrin receptor. *Journal of Virology* **77**: 1718–26.

Kaludov, N., Brown, K. E., Walters, R. W., Zabner, J. and Chiorini, J. A. 2001. Adeno-associated virus serotype 4 (AAV4) and AAV5 both require sialic acid binding for hemagglutination and efficient transduction but differ in sialic acid linkage specificity. *Journal of Virology* **75**: 6884–93.

Kaufmann, B., Simpson, A. A. and Rossmann, M. G. 2004. The structure of human parvovirus B19. *Proceedings of the National Academy of Sciences USA* **101**: 11628–33.

Kern, A., Schmidt, K., Leder, C. *et al.* 2003. Identification of a heparin-binding motif on adeno-associated virus type 2 capsids, *Journal of Virology* **77**: 11072–81.

Kimsey, P. B., Engers, H. D., Hirt, B. and Jongeneel, C. V. 1986. Pathogenicity of fibroblasts- and lymphocyte-specific variants of minute virus of mice. *Journal of Virology* **59**: 8–13.

Kleinschmidt, J. 2004. Dual function of capsid pore-forming proteins of parvovirus AAV2. *FASEB Summer Research Conference*. S-7.

Kresse, J. I., Taylor, W. D., Stewart, W. W. and Fernisse, K. A. 1985. Parvovirus infection in pigs with necrotic and vesicle-like lesions. *Veterinary Microbiology* **10**: 525–31.

Kronenberg, S., Kleinschmidt, J. A. and Böttcher, B. 2001. Electron cryo-microscopy and image reconstruction of adeno-associated virus type 2 empty capsids. *EMBO Reports* **2**: 997–1002.

Langeveld, J. P., Casal, J. I., Vela, C. *et al.* 1993. B-cell epitopes of canine parvovirus: distribution on the primary structure and exposure on the viral surface. *Journal of Virology* **67**: 765–72.

Langeveld, J. P., Casal, J. I., Cortes, E. *et al.* 1994. Effective induction of neutralizing antibodies with the amino terminus of VP2 of canine parvovirus as a synthetic peptide. *Vaccine* **12**: 1473–80.

Llamas-Saiz, A. L., Agbandje-McKenna, M., Parker, J. S. L., Wahid, A. T. M., Parrish, C. R. and Rossmann, M. G. 1996. Structural analysis of a mutation in canine parvovirus which controls antigenicity and host range. *Virology* **225**: 65–71.

Lopez de Turiso, J. A., Cortes, E., Ranz, A. *et al.* 1991. Fine mapping of canine parvovirus B cell epitopes. *Journal of General Virology* **72**: 2445–56.

López-Bueno, A., Mateu, M. G. and Almendral, J. M. 2003. High mutant frequency in populations of a DNA virus allows evasión from antibody therapy in an immunodeficient host. *Journal of Virology* **77**: 2701–8.

López-Bueno, A., Bryant, N., Kontou, M., Rubio, M.-P., McKenna, R., Agbandje-McKenna, M. and Almendral, J. M. 2005. Genetic and structural analysis of the parvovirus MVM capsid binding site to the sialic component of a primary pathogenic receptor. *Journal of Virology.* (in preparation)

Maroto, B., Ramirez, J. C. and Almendral, J. M. 2000. Phosphorylation status of the parvovirus minute virus of mice particle: mapping and biological relevance of the major phosphorylation sites. *Journal of Virology* **74**: 10892–902.

Maroto, B., Valle, N., Saffrich, R. and Almendral, J. M. 2004. Nuclear export of the nonenveloped parvovirus virion is directed by an unordered protein signal exposed on the capsid surface. *Journal of Virology* **78**: 10685–94.

Maxwell, I. H., Spitzer, A. L., Maxwell, F. and Pintel, D. J. 1995. The capsid determinant of fibrotropism for the MVMp strain of minute virus of mice functions via VP2 and not VP1. *Journal of Virology* **69**: 5829–32.

McKenna, R., Olson, N. H., Chipman, P. R. *et al.* 1999. Three-dimensional structure of Aleutian mink disease parvovirus: Implications for disease pathogenicity. *Journal of Virology* **73**: 6882–91.

Mengeling, W. L. and Cutlip, R. C. 1975. Pathogenesis of *in utero* infection: experimental infection of 5-week-old porcine fetuses with porcine parvovirus. *American Journal of Veterinary Research* **36**: 1173–7.

Mengeling, W. L. and Cutlip, R. C. 1976. Reproductive disease experimentally induced by exposing pregnant gilts to porcine parvovirus. *American Journal of Veterinary Research* **37**: 1393–400.

Molitor, T. W. and Joo, H. S. 1990. Clinical and pathological features of porcine parvovirus-related disease and its diagnosis. In: P. Tijssen (ed.), *Handbook of Parvoviruses, vol. II.* Boca Raton, Fla.: CRC Press, pp. 135–150.

Opie, S. R., Warrington Jr, K. H., Jr., Agbandje-McKenna, M., Zolotukhin, S. and Muzyczka, N. 2003. Identification of amino acid residues in the capsid proteins of adeno-associated virus type 2 that contribute to heparan sulfate proteoglycan binding, *Journal of Virology* **77**: 6995–7006.

Padron, E., Bowman, V. D., Kaludov, N. *et al.* 2005. The structure of adeno-associated virus 4. *Journal of Virology* **79**: 5047–58.

Palermo, L., Hueffer, K. and Parrish, C. R. 2003. Residues in the apical domain of the feline and canine transferrin receptors control host-specific binding and cell infection of canine and feline parvoviruses. *Journal of Virology* **77**: 8915–23.

Parker, J. S. L. and Parrish, C. R. 1997. Canine parvovirus host range is determined by the specific conformation of an additional region of the capsid. *Journal of Virology* **71**: 9214–22.

Parker, J. S. L., Murphy, W. J., Wang, D., O'Brien, S. J. and Parrish, C. R. 2001. Canine and feline parvoviruses can use human or feline transferrin receptors to bind, enter, and infect cells. *Journal of Virology* **75**: 3896–902.

Parrish, C. R. 1991. Mapping specific functions in the capsid structure of canine parvovirus and feline panleukopenia virus using infectious plasmid clones. *Virology* **183**: 195–205.

Parrish, C. R., Aquadro, C. F. and Carmichael, L. E. 1988. Canine host range and a specific epitope map along with variant sequences in the capsid protein gene of canine parvovirus and related feline, mink and raccoon parvoviruses. *Virology* **166**: 293–307.

Parrish, C. R. and Carmichael, L. E. 1986. Characterization and recombination mapping of an antigenic and host range mutation of canine parvovirus. *Virology* **148**: 121–32.

Qing, K., Mah, C., Hansen, J., Zhou, S., Dwarki, V. and Srivastava, A. 1999. Human fibroblast growth factor receptor 1 is a coreceptor for infection by adeno-associated virus 2. *Nature Medicine* **5**: 71–7.

Rabinowitz, J. E., Rolling, F., Li, C. *et al.* 2002. Cross-packaging of a single adeno-associated virus (AAV) type 2 vector genome into multiple AAV serotypes enables transduction with broad specificity. *Journal of Virology* **76**: 791–801.

Ramírez, J. C., Fiaren, A. and Almendral, J. M. 1996. Parvovirus minute virus of mice strain I multiplication and pathogenesis in the newborn mouse brain are restricted to proliferative areas and to migratory cerebral young neurons. *Journal of Virology* **70**: 8109–16.

Reguera, J., Carreira, A., Riolobos, L., Almendral, J. M. and Mateu, M. G. 2004. Role of interfacial amino acid residues in assembly, stability, and conformation of a spherical virus capsid. *Proceedings of the National Academy of Sciences USA* **101**: 2724–9.

Rimmelzwaan, G. F., Carlson, J., UytdeHaag, F. G. and Osterhaus, A. D. 1990. A synthetic peptide derived from the amino acid sequence of canine parvovirus structural proteins which defines a B cell epitope and elicits antiviral antibody in BALB c mice. *Journal of General Virology* **71**: 2741–5.

Rosenfeld, S. J., Yoshimoto, K., Kajigaya, S. *et al.* 1992. Unique region of the minor capsid protein of human parvovirus B19 is exposed on the virion surface. *Journal of Clinical Investigations* **89**: 2023–9.

Saikawa.T, Anderson, S., Momoeda, M., Kajigaya, S. and Young, N. S. 1993. Neutralizing linear epitopes of B19 parvovirus cluster in the VP1 unique and VP1-VP2 junction regions. *Journal of Virology* **67**: 3004–9.

Sato, H., Hirata, J., Furukawa, M. *et al.* 1991a. Identification of the region including the epitope for a monoclonal antibody which can neutralize human parvovirus B19. *Journal of Virology* **65**: 1667–72.

Sato, H., Hirata, J., Kuroda, N., Shiraki, H., Maeda, Y. and Okochi, K. 1991b. Identification and mapping of neutralizing epitopes of human parvovirus B19 by using human antibodies. *Journal of Virology* **65**: 5485–90.

Segovia, J. C., Real, A., Bueren, J. A., Almendral, J. M. 1991. *In vitro* myelosuppressive effects of the parvovirus minute virus of mice (MVMi) on hematopoietic stem and committed progenitor cells. *Blood* **77**: 980–8.

Segovia, J. C., Bueren, J. A. and Almendral, J. M. 1995. Myeloid depression follows infection of susceptible newborn mice with the parvovirus minute virus of mice (strain i). *Journal of Virology* **69**: 3229–32.

Segovia, J. C., Gallego, J. M., Bueren, J. A. and Almendral, J. M. 1999. Severe leukopenia and dysregulated erythropoiesis in SCID mice

persistently infected with the parvovirus minute virus of mice. *Journal of Virology* **73**: 1774–84.

Simpson, A. A., Chipman, P. R., Baker, T. S., Tijssen, P. and Rossmann, M. G. 1998. The structure of an insect parvovirus (*Galleria mellonella* densovirus) at 3. 7 Å resolution. *Structure* **6**: 1355–67.

Simpson, A. A., Chandrasekar, V., Hebert, B., Sullivan, G. M., Rossmann, M. G. and Parrish, C. R. 2000. Host range and variability of calcium binding by surface loops in the capsids of canine and feline parvoviruses. *Journal of Molecular Biology* **300**: 597–610.

Simpson, A. A., Hébert, B., Sullivan, G. M. *et al.* 2002. The structure of the porcine parvovirus: comparison with related viruses. *Journal of Molecular Biology* **315**: 1189–98.

Smith, T. J. and Moser, A. 1997. Antibody-mediated neutralization of Picornaviruses. In: Chiu, W., Burnett, R. M., Garcea, R. L. (eds), *Structural Biology of Viruses*. New York: Oxford University Press, pp. 134–56.

Spalhotz, B. A. and Tattersall, P. 1983. Interaction of minute virus of mice with differentiated cells: strain-dependent target cell specificity is mediated by intracellular factors. *Journal of Virology* **46**: 937–9.

Strassheim, M. L., Gruenberg, A., Veijalainen, P., Sgro, J.-Y. and Parrish, C. R. 1994. Two dominant neutralizing antigenic determinants of canine parvovirus are found on the threefold spike of the virus capsid. *Virology* **198**: 175–84.

Summerford, C. M., Bartlett, J. S. and Samulski, R. J. 1999. A role for integrin $\alpha_v\beta_5$ in adeno-associated virus type 2 (AAV-2) infection. *Nature Medicine* **5**: 78–82.

Tattersall, P. and Bratton, J. 1983. Reciprocal productive and restrictive virus-cell interactions of immunosuppressive and prototype strains of minute virus of mice. *Journal of Virology* **46**: 944–55.

Tattersall, P., Shatkin, A. J. and Ward, P. 1977. Sequence homology between the structural polypeptides of minute virus of mice. *Journal of Molecular Biology* **111**: 375–94.

Thacker, T. C. and Johnson, F. B. 1998. Binding of bovine parvovirus to erythrocyte membrane sialylglycoproteins. *Journal of General Virology* **79**: 2163–9.

Tresnan, D. B., Southard, L., Weichert, W., Sgro, J.-Y. and Parrish, C. R. 1995. Analysis of the cell and erythrocyte binding activities of the dimple and canyon regions of the canine parvovirus capsid. *Virology* **211**: 123–32.

Truyen, U., Agbandje, M. and Parrish, C. R. 1994. Characterization of the feline host range and a specific epitope of feline panleukopenia virus. *Virology* **200**: 494–503.

Truyen, U., Evermann, J. F., Vieler, E. and Parrish, C. R. 1996. Evolution of canine parvovirus involved loss and gain of feline host range. *Virology* **215**: 186–9.

Tsao, T., Chapman, M. S., Agbandje, M. *et al.* 1991. The three-dimensional structure of canine parvovirus and its functional implications. *Science* **251**: 1456–64.

Vihinen-Ranta, M., Wang, D., Weichert, W. S. and Parrish, C. R. 2002. The VP1 N-terminal sequence of canine parvovirus affects nuclear transport of capsids and efficient cell infection. *Journal of Virology* **76**: 1884–91.

Walters, R., Agbandje-McKenna, M., Bowman, V. D. *et al.* 2004. Structure of adeno-associated virus serotype 5. *Journal of Virology* **78**: 3361–71.

Wikoff, W. R., Wang, G., Parrish, C. R. *et al.* 1994. The structure of a neutralized virus: Canine parvovirus complexed with neutralizing antibody fragment. *Structure* **2**: 595–607.

Wistuba, A., Kern, A., Weger, S., Grimm, D. and Kleinschmidt, J. A. 1997. Subcellular compartmentalization of adeno-associated virus type 2 assembly. *Journal of Virology* **71**: 1341–52.

Wobus, C. E., Hugle-Dorr, B., Girod, A., Petersen, G., Hallek, M. and Kleinschmidt, J. A. 2000. Monoclonal antibodies against the adeno-associated virus type 2 (AAV-2) capsid: epitope mapping and identification of capsid domains involved in AAV-2-cell interaction and neutralization of AAV-2 infection. *Journal of Virology* **74**: 9281–93.

Xie, Q., Bu, W., Bhatia, S., Hare, J., Somasundaram, T., Azzi, A. and Chapman, M. S. 2002. The atomic structure of adeno-associated virus (AAV-2), a vector for human gene therapy. *Proceedings of the National Academy of Sciences USA* **99**: 10405–10.

Xie, Q., Chapman, M. S. 1996. Canine parvovirus capsid structure, analyzed at 2.9 Å resolution. *Journal of Molecular Biology* **264**: 497–520.

Yoshimoto, K., Rosenfeld. S., Frickhofen, N. *et al.* 1991. A second neutralizing epitope of B19 parvovirus implicates the spike region in the immune response. *Journal of Virology* **65**: 7056–60.

Zádori, Z., Szelei, J., Lacoste, M. C. *et al.* 2001. A viral phospholipase A_2 is required for parvovirus infectivity. *Development Cell* **1**: 291–302.